Int. J. Appl. Comput. Math (2016) 2:303–313
DOI 10.1007/s40819-015-0061-7

ORIGINAL PAPER

Space–Time Coupled Finite Element Simulation of PECVD Reactor

Z. Dehghanifard[1] · A. R. Ahmadi[1] · A. R. Ganjovi[1] · M. A. Bolorizadeh[1]

Published online: 7 May 2015

Abstract In this paper, space–time distribution of nanoparticles, as predicted by the fluid model, is simulated using Galerkin based space–time coupled finite element methodology. The method is utilized to simulate the silane discharge process and the ensuing behavior of the affected particles as a function of time in a plasma enhanced chemical vapor deposition (PECVD) reactor. PECVD is a practical technique of producing thin silicon films. Simulation of this process, as modeled by a set of nonlinear partial differential equations, requires extensive resolution in time. An attempt at establishing a stable and convergent computational process was successful only when space–time coupled finite element methodology was utilized to simulate this problem. Details of the methodology along with results of a particular test case are presented.

Keywords Space–time coupled finite element · PECVD reactor · Radio frequency discharge · Silicon amorphous thin film

Introduction

Plasma enhanced chemical vapor deposition (PECVD) is a technique of producing nano-sized particles at low pressures and low temperatures. In this method, the plasma is generated using radio frequency (RF) power source [1,2]. Electrons' movement leading to ionization reactions

✉ A. R. Ahmadi
ahmadi.publications@gmail.com

Z. Dehghanifard
l_dehghanifard@yahoo.com

A. R. Ganjovi
a.ganjovi@kgut.ac.ir

M. A. Bolorizadeh
ma.bolorizadeh@kgut.ac.ir

1 Kerman Graduate University of Advanced Technology, Kerman, Iran

is the fundamental process in the reactor volume. Ionization and attachment reactions produce positive and negative charged particles. Hence, as the process evolves through time, new species with varying number density take part in the reactions, thereby producing radicals and neutrals after a short while. Various particles move towards the substrate and are deposited on it to form amorphous thin films. The resulting thin film is then incorporated into industrial devices; in particular, electronic devices, solar cells and thin film transistors for controlling liquid crystal display (LCD) panels [3,4].

In this work, silane is considered as the background gas, and it is assumed that gas density is uniform and remains constant during the process. Using the one-dimensional fluid model coupled with Poisson's equation to account for electric field potential, the time and space variations in particle density for different species can be modeled [1,2,5]. Here, space–time coupled finite element (STCFE) method is utilized to investigate particles' behavior during the discharge process.

STCFE framework was adopted to solve this problem because of the high rates that exist in density variations, a consequence of the high frequency of power source. Coupling of time and space in finite element interpolation allows one to establish a stable and convergent evolutionary process for this problem.

The model considered here assumes silane gas in the background without any material flux into the system. As expected, periodic concentration for certain species hold their pattern in time, thereby, indicating the absence of numerical diffusion in the computational process, i.e. no reduction in peaks or change in period of concentration at any spatial point. Furthermore, the computed results demonstrate the production and consumption of each participating species as a function of time, as well as deposition and accumulation of certain species.

Model Description

Main objective of this study is to simulate the effects of ionization and production of different particles during the discharge process in a PECVD reactor. The reactor model includes two parallel electrodes covered with substrate that are placed 2.7 cm apart. The first electrode is grounded while the other electrode is connected to a Radio frequency (RF) power source, producing a periodic electric field at 136 MHz. Inside the reactor, a glow discharge is produced between the two electrodes. Ionization as well as all other reactions takes place during this glow discharge. As the process proceeds in time, different particles are produced in the reactor volume [6]. Radicals such as SiH_2 and SiH_3 are deposited on the substrate, which play an important role in thin film's growth. However, Si_2H_5 and heavier radicals are rarely produced during the discharge, and hence are neglected from this model [7,8]. Here, only the most dominant reactions in the reactor volume are considered.

A one-dimensional fluid model stating the conservation of particle number density for each species, along with Poisson's equation modeling reactor's potential, can accurately describe the PECVD process [1,2].

The conservation law, which holds for all species involved, i.e. electrons, neutrals, charged particles, and radicals, can be stated as the following [1,2]:

$$\frac{\partial n_j}{\partial t} + \frac{\partial \Gamma_j}{\partial z} = S_j, \tag{1}$$

where n_j is the particle number density for species j, Γ_j is particle's flux, and S_j is a prescribed source or sink for particle j in the reactor volume. Reactions that take place during the discharge process lead to production or loss for each species. Hence, for every

Table 1 Reaction rates where p_0 is the atmospheric pressure and T_{gas} is 520 K

Chemical reaction	Reaction rate ($cm^{-3}\ S^{-1}$)
$H + SiH_4 \longrightarrow SiH_3 + H_2$	$2.8 \times 10^{-11} \exp(-1250/T_{gas})$
$H + Si_2H_6 \longrightarrow Si_2H_5 + H_2$	$1.6 \times 10^{-10} \exp(-1250/T_{gas})$
$H + Si_nH_{2n+2} \longrightarrow Si_nH_{2n+1} + H_2$	$2.4 \times 10^{-10} \exp(-1250/T_{gas})$
$SiH_4 + SiH_2 \longrightarrow Si_2H_6$	$2 \times 10^{-10}[1 - (1 + 0.0032\ p_0)^{-1}]$
$Si_nH_{2n+2} + SiH_2 \longrightarrow Si_{n+1}H_{2n+4}$	$4.2 \times 10^{-10}[1 - (1 + 0.0033\ p_0)^{-1}]$
$SiH_3^- + SiH_2^+ \longrightarrow SiH_3 + SiH_2$	1.2×10^{-7}
$SiH_3^- + Si_2H_4^+ \longrightarrow SiH_3 + 2SiH_2$	1×10^{-7}

reaction, the source term in (1) can be written as:

$$A + B \rightarrow C + D$$
$$S_{rec,\,c,\,D} = -S_{rec,\,A,\,B} = n_A n_B K_{rec}, \tag{2}$$

where K_{rec} is the rate of reaction between species A and B. Table 1 lists the reaction rates used here [1].

Particle flux term in conservation equation can be replaced by the drift-diffusion approximation, i. e.

$$\Gamma_j = \mu_j n_j E - D_j \frac{\partial n_j}{\partial z}, \tag{3}$$

where μ_j is the mobility coefficient for species j, which is zero for a neutral or a radical. D_j is the diffusion coefficient of species j, which accounts for particle flux due to particle collisions [1,5,6].

For the particular case considered here, species that play significant roles in ionization and recombination processes as well as the production of electrons and radicals are listed in Table 2.

The PECVD reactor consists of two parallel electrodes covered with substrate at different electric potential. Here, potential for the bottom electrode is zero and the top electrode is connected to a radio frequency power source. The applied potential, as a function of time, t, can be stated mathematically as:

$$V_{(z=L)} = V_{rf} \sin(2\pi t \upsilon_{rf}), \tag{4}$$

where V_{rf} is the amplitude and υ_{rf} is the angular frequency of the power source, which are set as $V_{rf} = 150$ volts and $\upsilon_{rf} = 136$ MHz (period of 7.35×10^{-9}) [1,5].

Finite Element Modeling

Finite element method offers a general computational framework for solving systems of differential equations effectively, regardless of nonlinearities or complexities of the system under consideration. In treatment of initial boundary value problems (IBVP), the common approach is to state the approximation for field variable $n_j(\chi, t)$ as:

$$n_j(\chi, t) = \sum_i N_{ij}(\chi)\phi_{ij}(t), \tag{5}$$

Table 2 Species used in the model

Species j	Name	Type
e^-	Electron	Elementary
H	Atomic hydrogen	Radical
H_2	Hydrogen molecule	Neutral
Si_2H_5	Silane	Radical
Si_2H_6	Disilane	Neutral
SiH_2	Silylidene	Radical
SiH_3	Silyl	Neutral
SiH_2^+	Silylidene cation	Positive ion
$Si_2H_4^+$	Disilanylidene cation	Positive ion
SiH_3^-	Silyl anion	Negative ion

where $N_{ij}(\chi)$ are the interpolation bases defined in terms of spatial coordinates. The interpolation coefficients φ_{ij}, also referred to as the degrees of freedom, are functions of time.

Based on the approximation given in (5) an IBVP is transformed to a finite set of initial value problems (IVP) in terms of φ_{ij} for which the coefficients are established using $N_{ij}(\chi)$ functions. The resulting set of IVP is usually solved using finite difference methods with proper numerical stabilizers.

In this approach, interpolant n_j is decoupled in space and time. The decoupled formulation works well for many common problems; i.e. a convergent and stable evolutionary process can be established for many IBVP.

As a first attempt, space–time decoupled formulation was employed to solve the problem at hand. However, the approach was not successful and a convergent solution could not be obtained regardless of the time-step size.

However, the space–time coupled formulation that was tried next, led to a convergent and stable computational process. Details of the coupled formulation are given next.

Space–Time Coupled Formulation

This formulation treats time as an additional independent variable when forming finite element interpolants for each species j, i.e.

$$n_j(z,t) = \sum_i N_{ij}(z,t)\phi_{ij} = \mathrm{N}_j.\Phi_j \tag{6}$$

Here, the one dimensional IBVP is solved over the two dimensional computational domain of (z, t) instead of two, one dimensional domains of z and t. Obviously, this formulation significantly increases the associated computational cost. However, for the problem at hand, the coupling that exists in finite element interpolation was found to be necessary for establishing a stable and convergent evolutionary process.

The weighted residual formulation utilized here is Galerkin based. After performing integration by parts on Eq. (1) with respect to z while considering Eq. (6) the resulting Galerkin weak form becomes,

$$\int_{t_0}^{t_f}\int_0^L \left(w_j \frac{\partial n_j}{\partial t} + D_j \frac{\partial w_j}{\partial z}\frac{\partial n_j}{\partial z} + \mu_j n_j \frac{\partial w_j}{\partial z}\frac{\partial V_j}{\partial z} \right) dzdt$$
$$= \int_{t_0}^{t_f}\int_0^L w_j S_j \, dzdt \quad \text{For all } j \text{ given in Table 2} \tag{7}$$

where, L is distance between the two electrodes, and $[t_0, t_f]$ is the range of integration over time.

The weighting function $w_j = w_j(z, t)$ based on Galerkin formulation becomes,

$$w_j = \delta_{\Phi_j}(n_j) = \mathrm{N}_j^T \tag{8}$$

Galerkin form of the diffusion model describing the imposed electric field, after integration by parts becomes,

$$\int_{t_0}^{t_f}\int_0^L \frac{\partial w}{\partial z}\frac{\partial V}{\partial z} dzdt$$
$$= \sum_j \int_{t_0}^{t_f}\int_0^L w q_j n_j \, dzdt \quad \text{with sum over all } j \text{ given in Table 2} \tag{9}$$

where, q_j is the electric charge for species j.

Evolutionary nature of the IBVP allows for incrementation the time-span $t_0 \leq t \leq t_f$. Hence, instead of considering the entire time domain at once, it is computationally more efficient to break the domain into time slabs of duration Δt_i such that $\sum \Delta t_i = t_f - t_0$. One must use care in selecting time slabs durations Δt_i, since the size of Δt_i and meshing of the corresponding time slab affect evolution's stability as well as convergence to the nonlinear solution.

For the problem at hand, data relevant to time slabs are listed in Table 3. The best level of interpolation and global continuity for time were found to be $P_t = 1$ and $C_t = 0$.

Numerical Study

The problem given here consists of eleven coupled nonlinear partial differential equations for which the Galerkin form is given by integrals in (7) and (9). These equations govern the time dependent nonlinear response of eleven field variables, also referred to as the dependent variables, which are number densities for the ten constituting materials given in Table 2, in addition to one dependent variable representing electric potential.

Casting the equivalent Galerkin weak form over the two-dimensional field of space z and time t can solve this system of equations. Spatial discretization and time stepping details are listed in Tables 3 and 4 respectively.

Discretization in space is done using 52 elements such that as one moves away from either boundary, element size increases by 30 %. Non-uniformity of the mesh allows us to capture boundary effects accurately. Time slabs are divided into two equal-sized elements except for the first slab which has three elements with lengths that increase by 20 % as one moves away from time t = 0; allowing for the effects of initial conditions to be captured more accurately.

In this work, it is assumed that at beginning of the process all particles' density is 10^{10} m^{-3}; and there are no flux boundaries i.e. no material enters or leaves the reactor at any time. Non-dimensionalization parameters used in scaling the equations are listed in Table 5.

Table 3 Time stepping and discretization

i	Δt_i (ns)	N_{tE}	Grade
1	0.66×10^{-10}	3	1.2
2–500	0.66×10^{-10}	2	1

Table 4 Space discretization

Δz_i(cm)	nE	Grade
0–1.35	26	1.3
1.35–2.7	26	1/1.3

Table 5 Non-dimensionalization variables

Variable with dimension	Non-dimensionalization coefficient	Dimensionless variable
$n_j(m^{-3})$	$N_j = 10^{10}$	u_j
Φ(potential) (V)	F = 1	w
t (s)	$t_c = 0.66 \times 10^{-5}$	τ
z (m)	$z_c = 0.12$	λ

Discussion

The electric field induced through reactor's boundaries produces plasmatic environment inside the reactor. Here, ions and electrons react quickly to changes in the electromagnetic field, with electrons being the most affected particles to the electric discharge. As seen in Fig. 1 electron density rises quickly to an order of 10^{13} on the boundaries. Electrons maintain the highest density throughout, as compared to other species that are present in the reactor. An important point that indicates the accuracy of this simulation is the fact that period of spatial accumulation is the same as the period of imposed electric field for all particles except for electrons. Electrons have a longer period of accumulation, about 10 % longer, which can be attributed to their loss of momentum due to collisions and their relatively small mass. Ions, which are the main contributors to production of radicals, accumulate on the boundary at the same frequency as the imposed field. Their peak density is about 10^{12}, which is an order of magnitude smaller than electron density. Figures 2, 3 and 4 show the periodic accumulation of positive ions on the electrode. Figure 5 shows periodic generation and consumption of Hydrogen atoms on the electrode, with a steady growth rate. The model, also predicts steady accumulation of neutral particles, Fig. 6, which is the main purpose of a PECVD reactor.

As noted earlier, comparison of the pile-up and discharge rates for electrons and ions reveals that the process is faster for ions than for the electrons.

Based on results shown in Fig. 5 density of certain radicals on the boundaries, grow steadily. Radicals are neutral in charge and play an important role in growth of thin layers on top of the sub-layers. As can be seen from Fig. 6, radicals grow on the boundary steadily but at a much lower rate and have much lower concentration of 10^{10}. However, ions and electrons accumulate faster on the boundaries; and have much higher concentrations of 10^{12} and 10^{13} respectively. This is to be expected since ions and electrons are produced through collisions facilitated by the induced electric field, whereas the radicals, being electrically

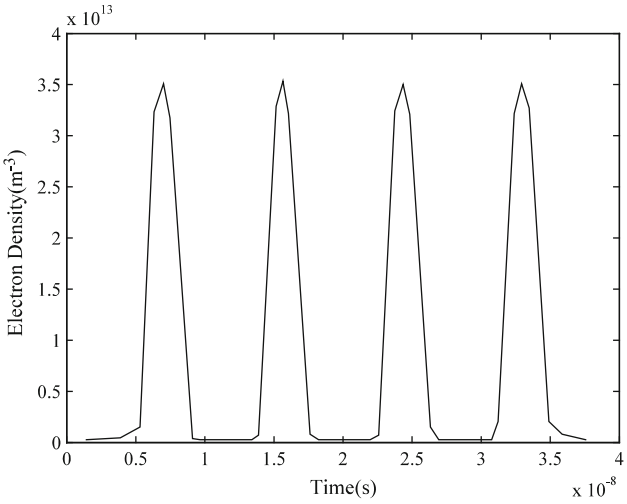

Fig. 1 Electron density changes at the electrode (Z = 2.7 cm)

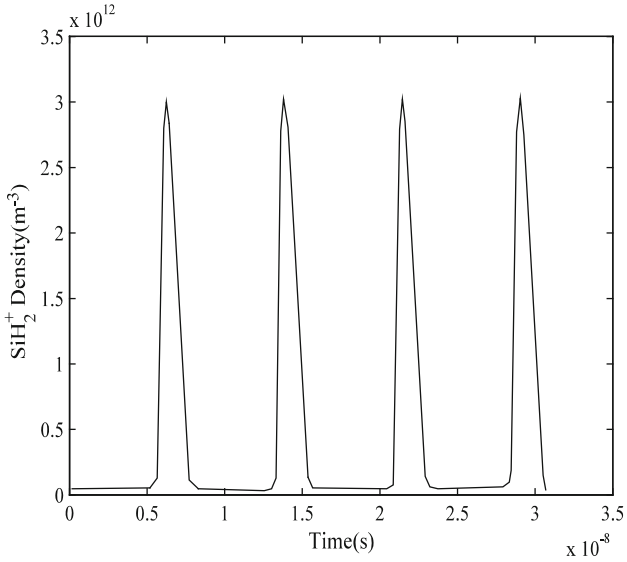

Fig. 2 SiH_2^+ Density changes at the electrode (Z = 2.7 cm)

neutral, are produced through chemical reactions. Neutral particles that do not participate in chemical reactions are deposited in thin layers on the boundaries; which is the main function of a PECVD reactor. Hydrogen radicals (H) react easily and are produced through different reactions. This property can be deduced from Fig. 5, on the boundaries H grows periodically at a steady rate. The much heavier radical, SiH_3, shown in Fig. 6 is non-reactive; it grows slowly and monotonically on the boundaries. The heavier radical of Si_2H_5 does not show any sign of growth due to its non-reactive nature; consequently Si_2H_5 has less effect on

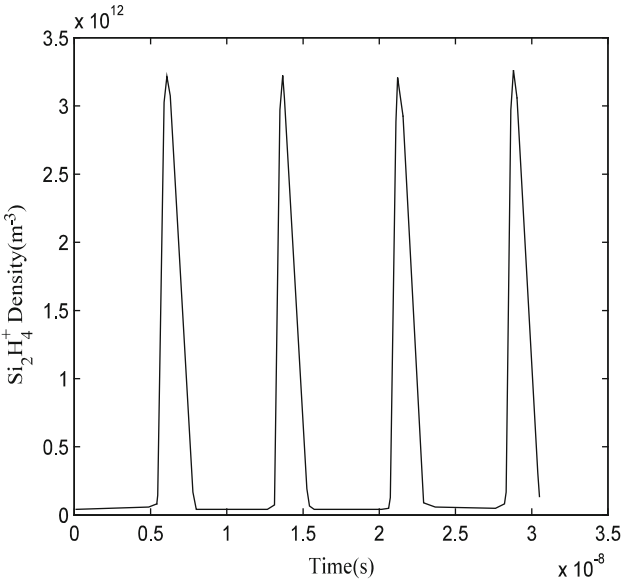

Fig. 3 $Si_2H_4^+$ Density changes at the electrode (Z = 2.7 cm)

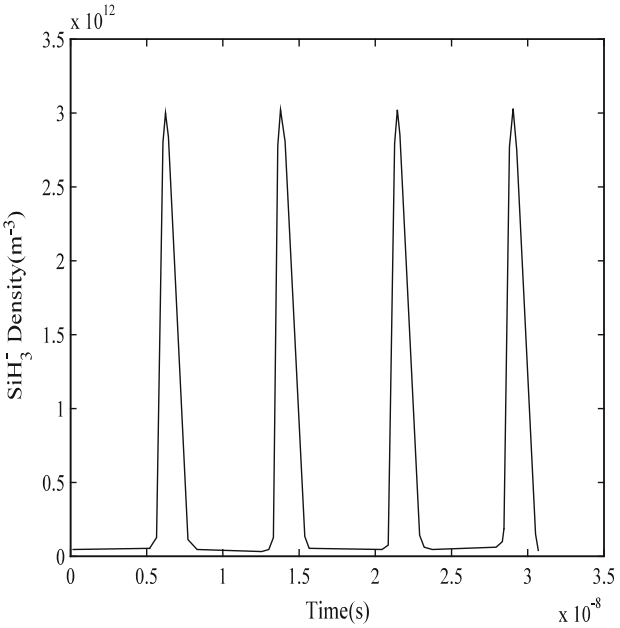

Fig. 4 SiH_3^- Density changes at the electrode (Z = 2.7)

production or deposition of layers on the boundaries and hence can be eliminated from the process. In another research effort, the effect of Si_2H_5 and heavier radicals are neglected completely [1].

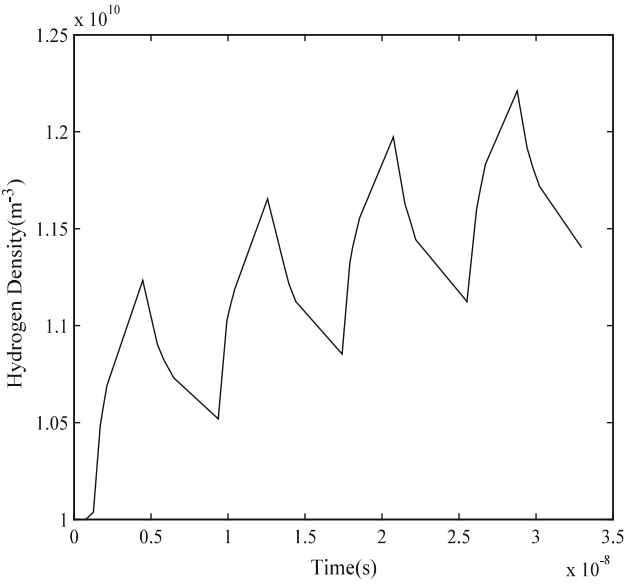

Fig. 5 Hydrogen density changes at the electrode (Z = 2.7 cm) Slope $= 62 \times 10^{15}$ m^{-3} s^{-1}

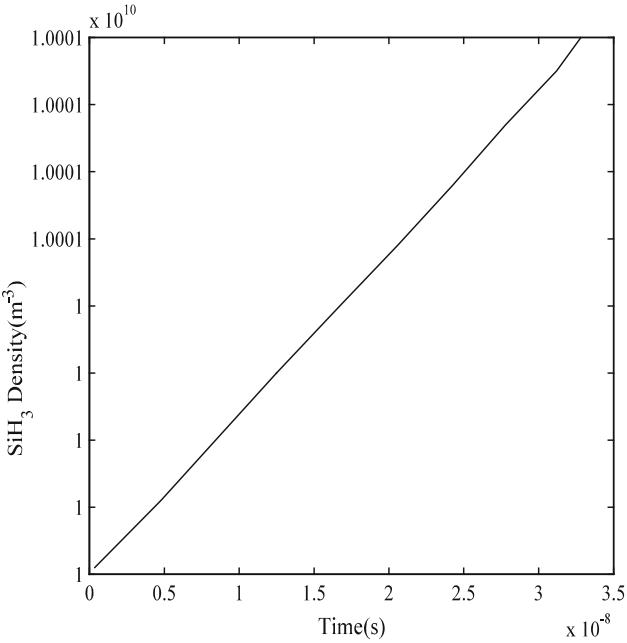

Fig. 6 SiH_3 density changes at the electrode (Z = 2.7 cm) Slope $= 5 \times 10^{13}$ m^{-3} s^{-1}

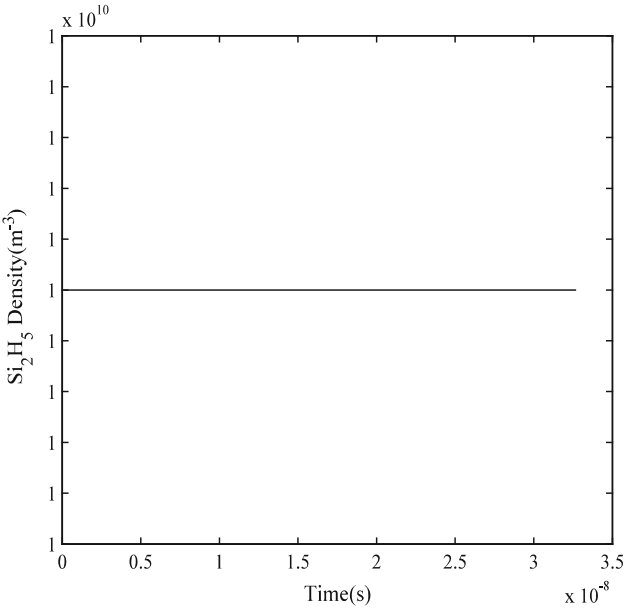

Fig. 7 Si_2H_5 density changes at the electrodes

Results Comparison

Even though our model is based entirely on the reactor-model utilized in [1], the results presented in that work are time-averaged quantities, over long periods, and cannot be compared with our high frequency time-resolved simulation. Nonetheless, in order to assess the correctness of our findings, published works of similar nature are referenced to validate the patterns that exist in our computed results.

Nanoparticle simulations carried out by Bleecker et al. [3] demonstrate that lighter particles deposit at higher densities. This pattern is consistent with the fact that lighter radicals are formed at a higher rate than heavier radicals; leading to higher density accumulations of lighter particles. This pattern is also evident from our simulations, Figs. 5, 6 and 7. Deposition of hydrogen radicals, Fig. 5, occurs at a higher rate than heavier radicals of SiH_3 and Si_2H_5, which successively have lower deposition rates and hence lower densities.

Another pattern matching is made through comparison with an experimental study [10] that is concerned with particle genesis and growth in RF silane plasmas. In this work, charged particles gather abruptly and disappear just as quickly; in a periodic manner. This pattern, with a minor difference, also exists in our computations of charged particles' densities, Figs. 1, 2, 3 and 4. Due to damping effects, wave patterns in [10] show decrease in amplitudes of consecutive peaks. The waves predicted by our numerical studies are abrupt and short-lived as well; however, they have no peak drops for the simple fact that the present mathematical model does not have any damping mechanism.

Furthermore, conservation of amplitude and shape of the computed waves are indicative of the dispersion-less nature of the computational process employed here. The space–time coupled finite element approximations are primarily responsible for the lack of numerical dispersion in the results. Inclusion of time as an additional dimension in the computational

domain, allows for correct representation of the nonlinearities that exist in this partial differential system of eleven equations.

Even though we cannot offer a one to one comparison with other similar works, we are able to assume validity of our results based on correctness of certain patterns that exist in our findings. Furthermore, correctness and effectiveness of the computational process can be concluded from dispersion-less nature of the results; and the fact that optimum interpolation order and mesh size were used here, i.e. any further improvements on mesh or interpolation order would not cause any significant change in computed results.

Conclusion

This paper has presented the space–time coupled finite element simulation of a PECVD reactor. Simulation of the high temporal gradients, due to the high frequency of RF input source, became possible when the formulation was based on space–time coupled Galerkin method. The coupled formulation leads to a stable and convergent evolutionary process. Computed results demonstrate the generation and periodic accumulation of participating particles. Ions accumulate on the boundaries at imposed frequency of the field, whereas electrons' accumulation frequency is lower because of their loss of momentum. The simulation also predicts a steady growth of neutral particles, SiH_3, which is the main purpose of a PECVD reactor.

References

1. Nienhuisa, G.J., Goedheer, W.J.: A self-consistent fluid model for radio-frequency discharges in SiH4-H2 compared to experiments. J. Appl. Phys. **82**, 2060–2069 (1997)
2. Lyka, B., Amanatides, E., Mataras, D.: Simulation of the electrical properties of SiH4/H2 RF discharges. Jpn. J. Appl. Phys. **45**, 8172–8176 (2006)
3. Bleecker, K.D., Bogaerts, A., Goedheer, W.J., Gijbels, R.: Modelling of formation and transport of nanoparticles in silane discharges. Phys. Rev. E **70**, 056407–0564014 (2004)
4. Camero, M., Gordillo-Vazquez, F.J., Gomez-Aleixandre, C.: Low-pressure PECVD of nanoparticles in carbon thin films from Ar/H2/C2H2 plasmas: synthesis of films and analysis of the electron energy Distribution Function. Chem. Vap. Depos. **13**, 326–334 (2007)
5. Bleecker, K.D., Herrebout, D., Bogaerts, A., Gijbels, R., Descamps, P.: One-dimensional modeling of a capacitively coupled RF plasma in silane/helium, including small concentrations of O2 and N2. J. Phys. D **36**, 1826–1833 (2003)
6. Akdim, M.R., Goedheer, W.J.: Modeling of dust in a silane/hydrogen plasma. J. Appl. Phys. **94**, 30–45 (2003)
7. Huanga, H., Winchester, K.J., Suvorova, A., Lawne, B.R., Liud, Y., Hud, X.Z., Dell b, J.M., Faraone, L.: Effect of deposition conditions on mechanical properties of low-temperature PECVD silicon nitride films. Mater. Sci. Eng. A **435–436**, 453–459 (2006)
8. Gorbachev, Y.E., Zatevakhin, M.A., Krzhizhanovskaya, V.V., Shveigert, V.A.: Special features of the growth of hydrogenated amorphous silicon in PECVD reactors. Tech. Phys. **45**, 77–86 (2000)
9. Ahmadi, A.R.: SyNA: An open architecture finite element system, user's mannual. Kerman Graduate University of Advanced Technology, Computational Mechanics Laboratory (2010)
10. Hollenstein, Ch., Dorier, J.L., Dutta, J., Sansonnens, L., Howling, A.A.: Diagnostics of particle genesis and growth in RF silane plasmas by ion mass spectrometry and light scattering. Plasma Sources Sci. Technol. **3**, 278–285 (1994)